ELSEVIER

International Journal of Solids and Structures 41 (2004) 1893–1909

INTERNATIONAL JOURNAL OF SOLIDS and STRUCTURES

www.elsevier.com/locate/ijsolstr

Singular stress fields near contact boundaries in a composite bolted joint

T.J. Whitney [a,*], E.V. Iarve [b], R.A. Brockman [a]

[a] *Aerospace Mechanics Division, University of Dayton Research Institute, 300 College Park Avenue, CSC-320, Dayton, OH 45469-0110, USA*

[b] *Non-Metallic Materials Division, University of Dayton Research Institute, 300 College Park Avenue, Dayton, OH 45469-0168, USA*

Received 24 April 2003; received in revised form 30 October 2003

Abstract

Singular stresses arising in the neighborhood of contact surfaces introduced in laminated orthotropic plates by mechanical joining with clamp-up were investigated by using local asymptotic solutions and full-field numerical analysis. Three-dimensional B-spline approximation of the displacements and a penalty function-based contact solution was used in the numerical analysis. Recent work has shown that fracture in bolted composite joints may initiate near the outer edge of the bolt head or washer away from the hole edge, particularly if the joint is preloaded. Material and geometric discontinuities exist in these regions, resulting in singular stress behavior. Asymptotic stress analysis was performed to obtain the power of singularity in these regions as a function of the bolt-head (washer) stiffness. Frictionless contact conditions were assumed. It was found that the characteristics of the stress singularity for such practically important combinations as titanium bolt-head and carbon fiber composite plate are similar to a crack in terms of the power of singularity and uniqueness of the singular term. Coefficients of the singular terms of the asymptotic expansion were determined by comparison with the numerical solution in the close vicinity of the singular contour. Good agreement between the asymptotic and numerical solution in the transition regions was observed.

Keywords: Composite materials; Stress singularity; Asymptotic solution; Bolted joint

1. Introduction

Fasteners have been the primary method of joining advanced composite materials since their introduction into mainstream aerospace applications in the mid-1960s. Design techniques for fastened joints have received considerable attention since that time due to the complex nature of the stress fields in the vicinity of the joint, the variety of failure modes that can occur, and the complexity of stress relieving mechanisms such as matrix cracking. Optimal bolted joint design requires a thorough understanding of two

* Corresponding author. Tel.: +1-937-229-3010; fax: +1-937-229-4235/4251.
E-mail address: whitney@udri.udayton.edu (T.J. Whitney).

0020-7683/$ - see front matter © 2003 Elsevier Ltd. All rights reserved.
doi:10.1016/j.ijsolstr.2003.11.013

important factors. First, the local stress field, including clamping forces, must be determined. Secondly, the development of damage and failure, and how localized damage influences the stress field, must be understood.

Recent advances in analysis and design of composite bolted joints typically have focused on areas of the joint at which damage might initiate, possibly leading to failure. Experimental observations have suggested several critical areas in such joints (Oplinger, 1996). These include the ply interface at the inside hole surface (whether or not the surface is in contact with the fastener shank); the corner formed by the inside hole edge and the top or bottom surface of the plate (which may be in contact with the bolt shank and the bolt-head or washer, respectively); and the outer edge of the bolt-head or washer where it contacts the top or bottom of the plate.

While the contact of the outer edge of the bolt-head with the composite plate has received less attention, the experimental evidence suggests this area should be of primary interest under certain conditions. For example, Smith et al. (1986) noted that washers in single-lap joints tend to "dig in" as the bolt and washer rotate under load, producing early damage in the loading cycle. Clip gauging suggested very little bending (due to eccentric loading of the single-lap joint) in the region under a torqued washer, but very high bending starting immediately at the washer edge. High bending and bolt rotation led to remote bearing failure at relatively low loads and caused the bolt to pull through the laminate if loading was continued. Eriksson (1990) demonstrated an increase in bearing strength with increasing clamping torque for both brittle and toughened epoxy matrix systems. Failures occurred at washer edges rather than adjacent to the contact point of the bolt and the laminate. Thus in the case of bolted connection, where clamp-up forces are exerted through the bolt-head (washer) it is the washer edge area away from the hole edge that requires detailed analysis for failure initiation prediction. Singular stress fields are expected to arise near these edges requiring asymptotic analysis.

Detailed three-dimensional analysis is required to assess the local stress fields around the bolt-head or washer. However, accurate stress calculation in the vicinity of a stress singularity is not easily achieved, even with a dense finite element mesh. An elasticity-based solution in the vicinity of the singular points is required to validate and verify the full-field numerical solution. In addition, determining the coefficients of the singular terms opens the possibility of applying a fracture mechanics-type approach to damage accumulation predictions.

Mikhailov (1978) appears to be the first to apply singularity analysis (in terms of asymptotic expansions) to laminated composite plates. Normal and tangential stresses were applied to two bonded wedges of different anisotropic materials and the degree of singularity at the vertex calculated. The procedure was applied to geometries representing a laminated plate free edge, and the degree of singularity at the interface of the plies and free edge was calculated (Mikhailov, 1979a,b). A polymeric/aluminum composite was also considered.

Wang and Choi (1982) used Lekhnitskii's complex stress function to construct a series solution to the same anisotropic wedge problem considered by Mikhailov. The multiplier (coefficient of the singular term) was determined by boundary collocation. This approach was later adapted into a singular, hybrid composite-wedge finite element (Wang and Yuan, 1983). Zwiers et al. (1982), using the Stroh formalism, found the stress near the free edge of an interface to include both exponential and logarithmic terms. Zwier's analysis provides all quantities except constants that must be determined by solving the complete problem with boundary conditions. Both types of singularities depend on stacking sequence. The exponential singularity depends on the boundary conditions, while the logarithmic singularity does not.

The results of asymptotic analysis at the ply interface in the straight free edge were first applied to open holes by Ericson et al. (1984). He assumed that the singular term of the asymptotic expansion at the hole edge was exactly the same as at the straight edge if the ply orientation, with respect to the direction tangential to the hole edge, is the same as the ply orientation in the straight edge problem. A special "hole element," combining the asymptotic and numerical approximation, was constructed. However, the singular

hole "elements," which combined a singular solution with a finite element solution, did not satisfy interlaminar traction continuity at the hole edge.

Folias (1989) developed an asymptotic solution for 3-D stresses near the interface between isotropic plies and the free edge of a hole. He extended the analysis to orthotropic laminates and found the power of the singularity to be dependent on location around the hole edge (Folias, 1992). For a graphite epoxy laminate the order of singularity was an order of magnitude lower than for the isotropic plates. The analysis also validated the assumptions Ericson used to estimate the power of the singularity around the hole.

Bar-Yoseph and Avrashi (1988) used a variational-asymptotic approach to analyze free-edge singularities. As the location of the singularity is approached, results indicated that the singularity is approximated by $\log r$ rather than $r^{-\alpha}$. Stolarski and Chiang (1989) examined laminates under axial stretching using "enriched" finite elements. The authors concluded that both the logarithmic and exponential singularities must be included if calculations of the singularity order were to be accurate. Reedy (1989) observed that the stress singularity of the form $r^{-\alpha}$ at the free edge of a typical laminate is rather weak.

Wang and Lu's (1993) asymptotic analysis developed an assumed displacement-based finite element including the singular asymptotic term for analyzing the singularity at a hole edge. The element was used only near the free edge of the hole. Within the development, they showed that the first term of the asymptotic expansion of the 3D elasticity problem, when expressed as a ratio of ply thickness to hole diameter, represented a 2D elasticity problem. However, the resulting eigenfunctions of the 2D solution do not satisfy the 3D equations in any finite volume.

Yang et al. (2003) developed a multilayer boundary element technique to analyze elastic pinned joints under bearing and bypass loading and including friction. Employing Green's functions satisfying interlaminar displacement and traction continuity, their method required discretization of only the hole surface. The effects of loading sequence, cyclic loading, and friction on stress states in the contact zone were examined. Reduced pressure in the contact zone was found to be offset by induction of significant shear traction on the hole surface.

Systematic investigation of the character of the singular stress fields in the vicinity of the open and filled holes in orthotropic laminates was performed by Iarve (1996, 1997, 2000). In the case of the filled hole (Iarve, 1997), the asymptotic solution was extended to three-body contact to obtain the powers of singularity arising at the ply interfaces and the hole edge in contact with elastic fastener as a function of the fastener stiffness. In the fastener hole and the open hole case only one singular term with real power of singularity was found and the stress fields obtained by using numerical analysis were shown to agree well with the one term asymptotic expansion with appropriate coefficients. Iarve and Pagano (2001) superimposed the asymptotic solution and a spline-based numerical solution to create a full-field singular stress solution for an open-hole laminate at the ply interface. Reissner's variational principle was used. Coarse out-of-plane and in-plane subdivisions were sufficient to accurately calculate the coefficients of the asymptotic solution, which resulted in converged interlaminar stresses. A similar approach was applied to develop a combined asymptotic numerical solution in the case of filled holes. The new technique was experimentally validated by Iarve and Mollenhauer (2002) using the Moiré interferometry technique. With the exception of the interlaminar normal component, the analytically calculated and experimentally measured strains agreed very well for the $[+30_2/-30_2/90_4]_{3S}$ laminate considered. In the case of the interlaminar normal strain, however up to 20% difference in the stress amplitude was reported between the experiment and prediction, though the shape of the distributions were very similar.

The objective of this work is to extend the latter approach beyond the open and pin-filled hole problems to consider bolted joints with clamp-up. The singularities at the hole edge will be affected by the presence of the bolt-head only through the multiplicative terms defined by the far-field solution, whereas the singular terms and powers of singularity will remain unaffected. In accordance with experimental evidence (Oplinger, 1996; Smith, 1986; Eriksson, 1990), the present study will focus on the new phenomenon introduced by the bolt-head and clamp-up, namely the stress singularities under the bolt-head edge away

from the hole edge where contact with the surface of the plate occurs. The power of the singularity existing at the outer edge of the bolt-head will be calculated for boundary conditions representing frictionless contact of the bolt-head with the composite plate. The multiplicative coefficients of the singular term will be calculated by comparing the asymptotic expansion to a numerical full-field analysis. The resulting analysis can be applied to composite bolted joint designs using arbitrary lay-ups and a very general class of fasteners, to understand the local stress distribution and improve reliability and part life.

2. Problem statement

An idealized geometry representing the bolt-head and laminate is shown on Fig. 1. An n-ply composite plate of length X_L, width Y_L, and thickness H, contains a hole of diameter D_{hole} located at coordinates (x_c, y_c). A bolt with shank diameter D_{bolt}, head diameter d, and head thickness t_{bh} is centrally located in the hole. Although in general $D_{hole} \neq D_{bolt}$ (clearance or press-fit is possible), $D_{hole} = D_{bolt}$ in the present work. Mid-plane symmetry is assumed, restricting the numerical solution to double-lap joints and symmetric laminate stacking sequences. These restrictions can be lifted readily at the expense of large computational costs.

The loading conditions are applied via displacement boundary conditions at plate edges

$$u_y(XL, y, z) = 0, \quad u_x(XL, y, z) = u_0 \tag{1}$$

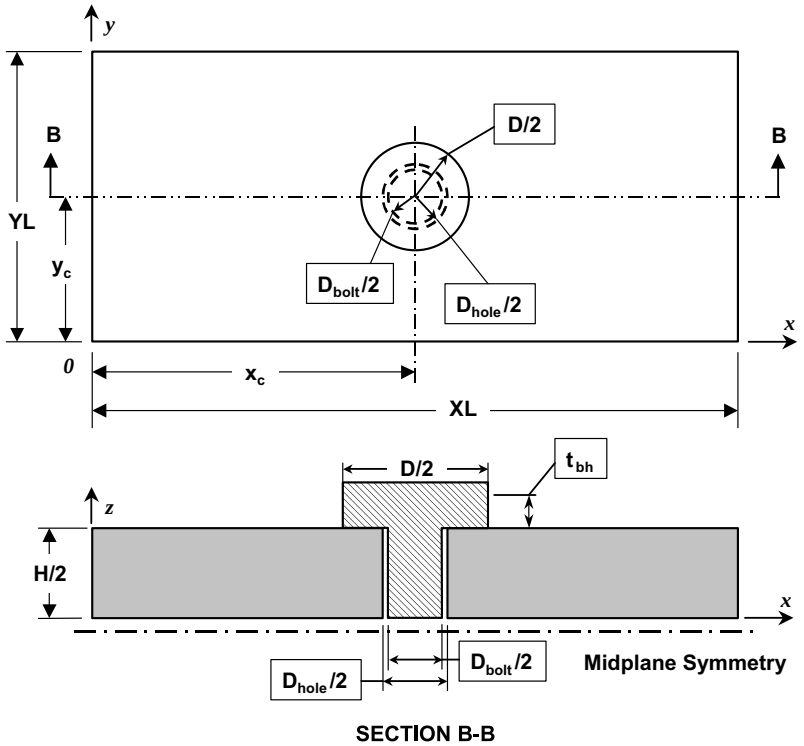

Fig. 1. Idealized geometry representing bolt-head and laminate.

Mid-surface symmetry conditions require

$$u_z(x, y, 0) = 0 \tag{2}$$

The top center of the bolt-head is constrained in the in-plane directions, so the applied displacement u_0 generates bearing loading. Clamp-up force is simulated by applying a displacement δ_y to the mid-surface of the bolt shank. All other facial surfaces are traction free. The constitutive relations in each ply are as follows:

$$\sigma_{ij} = C^p_{ijkl}(\varepsilon_{kl} - \alpha^p_{kl}\Delta T) \tag{3}$$

where C^p_{ijkl} and α^p_{kl} are elastic moduli and thermal expansion coefficients of the p-th orthotropic ply, and ΔT is the temperature change.

2.1. Asymptotic analysis

The location under consideration is at the outer diameter of the fastener head where it contacts the surface of the composite, Fig. 2. A local curvilinear coordinate system η, ψ, θ is established at the fastener head edge with the circumferential coordinate direction θ proceeding counterclockwise from the x-axis and the local orientation angle ψ proceeding counterclockwise from the free surface of the plate. The variable η is a distance from the plate–bolt-head corner, normalized by the bolt-head radius.

The transformation between the global and local coordinate systems is given by:

$$x = \frac{d}{2}(1 + \eta\cos\psi)\cos\theta \tag{4}$$

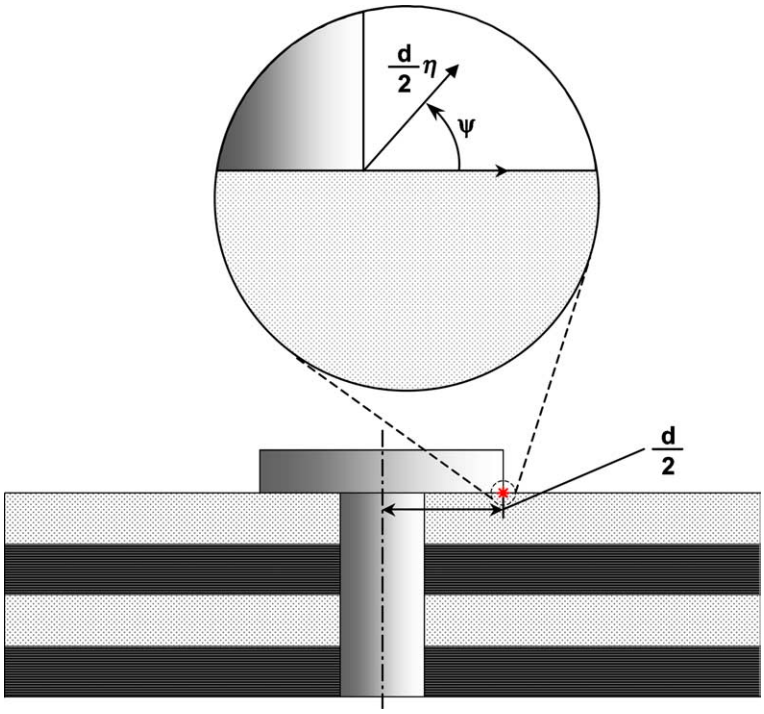

Fig. 2. Local curvilinear coordinate system.

$$y = \frac{d}{2}(1 + \eta\cos\psi)\sin\theta \tag{5}$$

$$z = \frac{d}{2}\eta\sin\psi + H/2 \tag{6}$$

Using the chain rule of differentiation and the Jacobian of the transformation, one can show that for an arbitrary function $F = F(\eta, \psi, \theta)$,

$$\frac{\partial F}{\partial x} = \frac{2}{d}\left\{\cos\theta\left[\frac{\partial F}{\partial \eta}\cos\psi - \frac{\partial F}{\partial \psi}\frac{\sin\psi}{\eta}\right] - \frac{\sin\theta}{(\eta\cos\psi + 1)}\frac{\partial F}{\partial \theta}\right\} \tag{7}$$

$$\frac{\partial F}{\partial y} = \frac{2}{d}\left\{\sin\theta\left[\frac{\partial F}{\partial \eta}\cos\psi - \frac{\partial F}{\partial \psi}\frac{\sin\psi}{\eta}\right] - \frac{\cos\theta}{(\eta\cos\psi + 1)}\frac{\partial F}{\partial \theta}\right\} \tag{8}$$

$$\frac{\partial F}{\partial z} = \frac{2}{d}\left[\frac{\partial F}{\partial \eta}\sin\psi + \frac{\partial F}{\partial \psi}\frac{\cos\psi}{\eta}\right] \tag{9}$$

Following Iarve (1996), one notes that the first two terms in (7) and (8) are of the order F/η (designated $\theta(F/\eta)$) while the third term (containing the θ-derivative) is $\theta(F)$. Therefore the terms containing $\partial F/\partial\theta$ in (7) and (8) can be neglected as $\eta \to 0$, with the acknowledgement that the equations are exact only in the asymptotic sense. The following operators are defined based on the relationships above:

$$\Lambda_t = \cos\psi\frac{\partial}{\partial\eta} - \frac{\sin\psi}{\eta}\frac{\partial}{\partial\psi} \tag{10}$$

$$\Lambda_n = \sin\psi\frac{\partial}{\partial\eta} + \frac{\cos\psi}{\eta}\frac{\partial}{\partial\psi} \tag{11}$$

Using these definitions, the equilibrium equations in the (x, y, z) coordinate system can be expressed as

$$\{\mathbf{F}\Lambda_t\Lambda_t + \mathbf{G}\Lambda_t\Lambda_n + \mathbf{H}\Lambda_n\Lambda_n\}\begin{Bmatrix} u_x \\ u_y \\ u_z \end{Bmatrix} = 0 \tag{12}$$

The matrices **F**, **G**, and **H** are functions of the elastic constants and coordinate θ and are given in the Appendix A.

The solution to (12) can be shown to have the form:

$$\begin{Bmatrix} u_x \\ u_y \\ u_z \end{Bmatrix} = \eta^{\lambda}(\sin\psi + \mu\cos\psi)^{\lambda}\begin{Bmatrix} d_x \\ d_y \\ d_z \end{Bmatrix} \tag{13}$$

in which $\mathbf{d} = (d_x, d_y, d_z)$, μ, and λ are arbitrary complex constants. Substituting (13) into (12) provides a sixth-order characteristic equation, which yields values for μ and the corresponding eigenvectors **d**. The general solution to (12) is a linear combination of the forms (13) associated with each of the six eigenvalues μ:

$$\mathbf{u} = \sum_{k=1}^{6} f_k\mathbf{d}_k\eta^{\lambda}(\sin\psi + \mu_k\cos\psi)^{\lambda} \tag{14}$$

in which $\mathbf{d}_k$ is the eigenvector associated with μ_k. Expressions for stress can be found by substituting (14) into Hooke's law written in terms of displacement:

$$\sigma_i = \lambda\eta^{\lambda-1}\sum_{k=1}^{6}\Big[f_k(\sin\psi+\mu_k\cos\psi)^{\lambda-1}\big([(C_{i1}\cos\theta+C_{i6}\sin\theta)\mu_k+C_{i5}]d_k^x + [(C_{i2}\sin\theta+C_{i6}\cos\theta)\mu_k+C_{i4}]d_k^y+[(C_{i4}\sin\theta+C_{i5}\cos\theta)\mu_k+C_{i3}]d_k^z\big)\Big], \tag{15}$$

where contracted notations are used, so that $(\sigma_i;\ i=1,2,\ldots,6)$ correspond to σ_{xx}, σ_{yy}, σ_{zz}, σ_{yz}, σ_{xz}, and σ_{xy}, respectively, C_{ij}, $i,j=1,\ldots,6$ are the components of the elasticity matrix in contracted notation, and $d_k^x d_k^y d_k^z$ are the components of $\mathbf{d}_k$. Material symmetry eliminates a number of terms in (15). For example, a material with its z-axis perpendicular to a plane of symmetry (such as a unidirectional composite ply) has $C_{14}=C_{15}=C_{24}=C_{25}=C_{34}=C_{35}=C_{46}=C_{56}=0$. The only unknown quantities in Eqs. (11) and (12) are the values of the power of singularity λ and coefficients f_k, $k=1,\ldots,6$. These quantities are found from the boundary conditions at material interfaces and free edges. Six boundary conditions can be written at the material interface $\psi=\pi$ and three at each of the free edges $\psi=0,\pi/2$. For the frictionless boundary conditions between the bolt-head and the plate:

$$\sigma_3^{(1)}=\sigma_4^{(1)}=\sigma_5^{(1)}=0,\quad \psi=0,\pi/2$$

$$\left.\begin{array}{l}\sigma_3^{(1)}=\sigma_3^{(2)}\\ u_3^{(1)}=u_3^{(2)}\\ \sigma_4^{(1)}=\sigma_5^{(1)}=0\\ \sigma_4^{(2)}=\sigma_5^{(2)}=0\end{array}\right\}\quad \psi=\pi \tag{16}$$

Substituting the expressions for displacement (14) and stress (15) into the boundary conditions (16) yields a system of 12 homogeneous equations with 12 unknowns. Non-trivial solutions exist if the determinant of the coefficient matrix vanishes, which occurs only for specific values of the exponent λ. An LU-decomposition algorithm (Press et al., 1989) is used to calculate the determinant, along with Muller's method (Gerald and Wheatley, 1994) for finding the λ roots. There are an infinite number of λ's that qualify, including all integers (Iarve, 1996). Once a value of λ is obtained, values of f_k for each material are determined as eigenvectors of the 12 by 12 system of equations. They are defined with accuracy to an undetermined multiplicative factor, which is a function of the circumferential coordinate θ only. The stress components can be represented by a linear combination of all solutions associated with the λ's:

$$\sigma_k = \sum_{j=1}^{\infty} S_j(\theta)\lambda_j\eta^{\lambda_j-1}\bar{\sigma}_k^{(j)}(\lambda_j,\psi,\theta)+\mathrm{O}(\eta^{\lambda_1}) \tag{17}$$

The factors $S_j(\theta)$ are the undetermined multiplicative coefficients to be found using a far-field solution that accounts for externally applied loads and constraints. The undefined additive $\mathrm{O}(\eta^{\lambda_1})$, where $\mathrm{Re}(\lambda_1)>0$ and λ_1 is the smallest root (dominating singular root), appears because only a single term is retained in the expansion about η in (5)–(7). The presence of such terms prohibits using expansion (17) to approximate the exact 3-D elastic solution even if we were to include a large amount of terms. The restriction is the consequence of the curvature of the singular contour as it proceeds around the edge of the bolt-head. In the following we will be interested in the singular roots $0<\mathrm{Re}(\lambda)<1$ and all roots $\mathrm{Re}(\lambda)<\mathrm{Re}(\lambda_1+1)$.

Our goal will be to define a region in the vicinity of the singularity in which the full-field numerical solution can be matched with a one or more term asymptotic expansion by appropriately choosing coefficients $S_j(\theta)$. If this region is sufficiently close to the singular contour then the contribution of the omitted terms in series (17) will be small and provide accurate values of coefficients of the initial terms of the asymptotic expansion.

2.2. Full-field numerical solution

The full-field solution could be obtained by any method that satisfies the external boundary conditions, including finite element analysis and/or boundary element analysis. In the present work the full-field solution was obtained by using a spline-based approximation of the displacements within a minimum potential energy formulation.

2.2.1. B-spline displacement approximation in unit volume

Consider an elementary volume $[0,1]^3$ and a set of piecewise polynomial 3-D functions $X_i(\mathbf{x})$ which provide partition of unity-type basis functions for displacement approximation, so that

$$\mathbf{u}(\mathbf{x}) = \sum X_i(\mathbf{x})\mathbf{U}_i \tag{18}$$

in which $\mathbf{U}_i$ are displacement approximation coefficients not necessarily associated with nodal displacements, and index i in (18) varies from 1 to the total number of approximation functions, which we will denote as a set $\mathbf{\Omega}$.

Three-dimensional shape functions $X_i(\mathbf{x})$ in approximation (16) are constructed from one-dimensional sets of B-spline basis functions of order n and defect k as standard tensor products, where the power of the spline is defined by the maximum power of the polynomials used to construct the spline, and the defect k defines the maximum number of discontinuous derivatives at a node, where $1 \leqslant k \leqslant n$. Practical usefulness of the spline approximation for solution of boundary value problems is determined by the properties of the set of basis functions used in the analysis. The B-spline basis functions, possessing the shortest possible support for a given power n and defect k, represent an attractive choice (see Iarve (1996) and references therein). A set of cubic ($n = 3$) B-spline basis functions with defect $k = 1$ built over seven subdivisions is shown in Fig. 3. The minimum support length property provides maximum sparsity of the resulting system of equations. Another significant advantage of the B-spline basis is the ability to change the defect of the spline at the end nodes. This allows one to build a system of basis functions such that the displacements at the end nodes are the actual coefficients of the spline functions, providing a convenient way of imposing

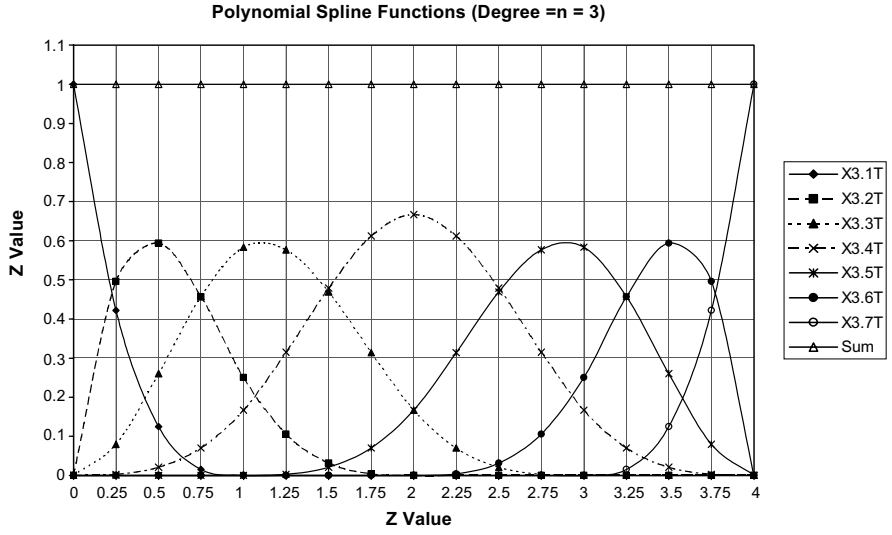

Fig. 3. Cubic spline over four intervals.

boundary conditions by simply assigning spline function coefficients analogous to a traditional finite element approximation. It should be noted that the displacements in the internal nodes are not explicitly equal to the coefficients of the B-spline functions.

A recurrence relationship based on polynomial representation (Iarve, 1996) was used to build the set of B-spline basis functions of arbitrary order and defect. Each one-dimensional basis spline function is non-negative and possesses local support of no more than $n-k+2$ nodal intervals. These one-dimensional basis functions, as well as multidimensional ones obtained as a tensor product of one-dimensional splines, represent a partition of unity with unit coefficients:

$$\sum_{i\in\Omega} X_i(\mathbf{x}) \equiv 1, \quad \mathbf{x} \in [0,1]^3 \tag{19}$$

2.2.2. Approximation in arbitrary volume

Approximation (17) is applied piecewise in volume partitions of the structure of interest, so that each of the partitions can be conformably mapped onto the unit volume $[0,1]^3$. In the case of B-spline approximation, the boundaries between these regions will be the only surfaces of C^0 displacement continuity, whereas inside this volume the displacement approximation smoothness is defined by the defect of the spline approximation. It is therefore desired to have large and few partitions. This is not always the case with traditional p-type approximations, where only the power of approximation can be increased to achieve given accuracy after the elements are defined. Curvilinear transformations $x = \boldsymbol{\eta}_j(\boldsymbol{\varsigma})$ are defined for each subvolume to map their physical volume into the unit volume, so that the displacement approximation in global (x,y,z) coordinates can be written:

$$\mathbf{u}^{(j)}(\mathbf{x}) = \sum_{i\in\Omega_j} X_i^{(j)}(\boldsymbol{\varsigma})\mathbf{U}_i^{(j)}, \quad \mathbf{x} = \boldsymbol{\eta}_\mathbf{j}(\boldsymbol{\varsigma}) \tag{20}$$

where $\boldsymbol{\varsigma} \in [0,1]^3$ and the sets of indexes Ω_j, $j = 1,\ldots,N$ correspond to individual subvolumes.

The penalty function approach, along with the notion of a contact surface characteristic function (Whitney and Iarve, 2002), is used to formulate the contact problem between the fastener and the plate. Frictionless contact is assumed.

2.2.3. Far-field model discretization

The spline mesh used in the plate and bolt are shown in Fig. 4. Total of $N = 38$ subvolumes, shown in different shades of gray were used, with C^0 continuity of displacements between adjacent subvolumes. White lines indicate the internal mesh in the subvolumes, where displacement continuity is defined by the defect of the spline approximation. Cubic splines with defect $k = 1$ were used in the analysis, yielding twice continuously differentiable displacement fields defining the overlapping splines. The close-up in Fig. 5 highlights the non-uniform distribution of mesh intervals that reduces the interval length near the points of interest, i.e., the edge of the bolt-head. Contact surfaces are also highlighted.

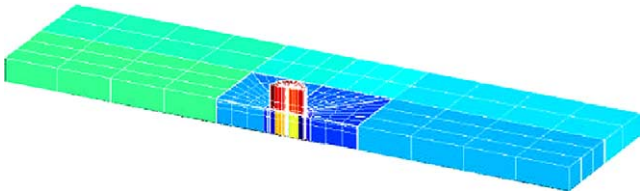

Fig. 4. BSAM mesh used in far-field analysis.

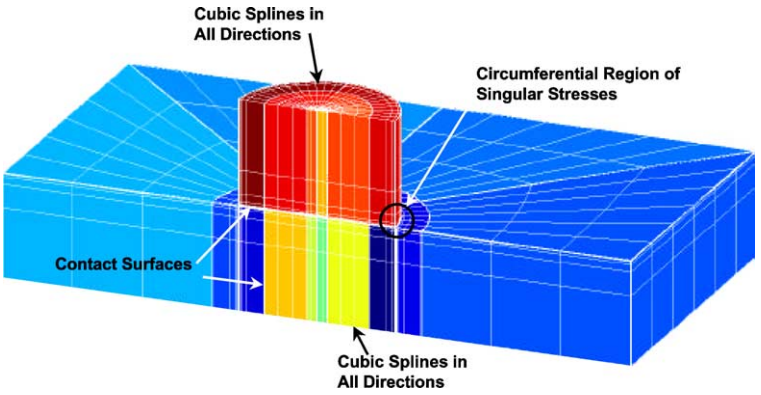

Fig. 5. BSAM mesh details for bolt–plate interaction.

3. Results and discussion—stress singularity

The asymptotic solution procedure described has been applied to the washer-edge configuration using the material properties shown in Table 1. Material 1 is assumed to consist of an orthotropic 0-degree ply with properties typical of an aerospace-grade high-modulus graphite/epoxy prepreg. Material 2, representing the fastener head, is assumed to consist of an isotropic material. Several fastener materials of varying stiffness have been used in the calculation, including a generic thermoplastic-bearing material denoted by "TPB" in Table 1. Because the solution form (14) is valid for all-distinct values of μ_k, and isotropic materials exhibit two distinct roots ($\pm i$) of triple multiplicity, the properties of Material 2 are made slightly orthotropic. X-direction properties have been marginally increased by an "orthotropy factor" denoted ε, of magnitude 10^{-7}, creating transverse isotropy in the $y-z$ plane:

$$\begin{aligned} &E_1 = (1+\varepsilon)E, \quad E_2 = E, \quad E_3 = E \\ &G_{23} = \frac{E}{2(1+\nu)}, \quad G_{13} = (1+\varepsilon)G_{23}, \quad G_{12} = (1+\varepsilon)G_{23} \\ &\nu_{23} = \nu, \quad \nu_{13} = (1+\varepsilon)\nu, \quad \nu_{12} = (1+\varepsilon)\nu \end{aligned} \tag{21}$$

Table 1
Material properties in washer-edge singularity analysis

	High-modulus graphite/epoxy	303 Steel	7075-T6 Aluminum	Grade 12 Titanium	Generic TPB
E (GPa)	–	193.0	71.7	105.0	3.45
ν	–	0.25	0.33	0.34	0.35
ε	–	1×10^{-7}	1×10^{-7}	1×10^{-7}	1×10^{-7}
E_1 (GPa)	139.0	193.0000193	71.70000717	104.8000105	3.450000345
E_2 (GPa)	10.34	193.0000000	71.70000000	104.8000000	3.450000000
E_3 (GPa)	10.34	193.0000000	71.70000000	104.8000000	3.450000000
G_{23} (GPa)	3.31	77.20000000	26.95488722	39.10447761	1.277777778
G_{13} (GPa)	5.52	77.20000772	26.95488991	39.10448152	1.277777906
G_{12} (GPa)	5.52	77.20000772	26.95488991	39.10448152	1.277777906
ν_{23}	0.55	0.2500000000	0.3300000000	0.340000000	0.350000000
ν_{13}	0.30	0.2500000250	0.3300000330	0.340000034	0.350000035
ν_{12}	0.30	0.2500000250	0.3300000330	0.340000034	0.350000035

This approach has been shown to yield accurate results for filled—hole edge singularities between isotropic materials (Iarve, 1997).

3.1. Singularity exponent and angular distribution of stress amplitudes

Fig. 6 shows the singularity exponent at the bolt-head edge as a function of circumferential position around the hole for steel, aluminum, titanium, and TPB bolt-head materials, for a slip condition at the interface (no shear tractions at the material interface). The results were obtained for 0° composite ply. Note that the results for other surface ply orientations can be generated by simple horizontal shift of the curves on Fig. 6, due to isotropic properties of the bolt-head. At each location only one purely real root is found. As expected, the power of singularity ($\lambda - 1$) weakens with reduced stiffness of the bolt-head, ranging from almost crack-like ($\lambda \sim -0.53$) to free-edge like singularities ($\lambda - 1$) ~ -0.15 for TPB.

In aerospace applications the practical range of bolt-head stiffnesses is between aluminum and steel, with the most common bolt-head material being titanium. For this range of materials the power of singularity is very close to −0.5, is limited to one real root, and exhibits only small circumferential variation. These characteristics resemble those of a crack in linear fracture mechanics. Therefore the question of determining the multiplicative coefficient $S_1(\theta)$ in Eq. (17) is of significant interest. Experimental work, required to further investigate whether a single parameter $S_1(\theta)$ can be validated to control the bolt-head edge shear-in failure, extends beyond the scope of present work. The remainder of this paper concentrates on comparison of the stress fields resulting from the singular term of the asymptotic solution and the full-field numerical solution in order to obtain $S_1(\theta)$.

The angular distributions of the stress amplitudes $\bar{\sigma}_k^{(1)}(\lambda_1, \psi, \theta)$ as functions of ψ are shown in Fig. 7 at four circumferential θ locations. All stress components are transformed into the local (η, ψ, θ) coordinate system. A steel bolt-head was examined. Stress amplitudes were normalized so that $\bar{\sigma}_{\psi\psi}^{(1)}(\lambda_1, 180°, \theta) = 1$. The range $90° \leqslant \psi < 180°$ of the angular coordinate is inside the bolt-head and $180° < \psi \leqslant 360°$ is inside the composite layer. The stress amplitudes satisfy the boundary conditions (16): $\bar{\sigma}_{\psi\psi}^{(1)}(\lambda_1, \psi, \theta)$ is continuous at

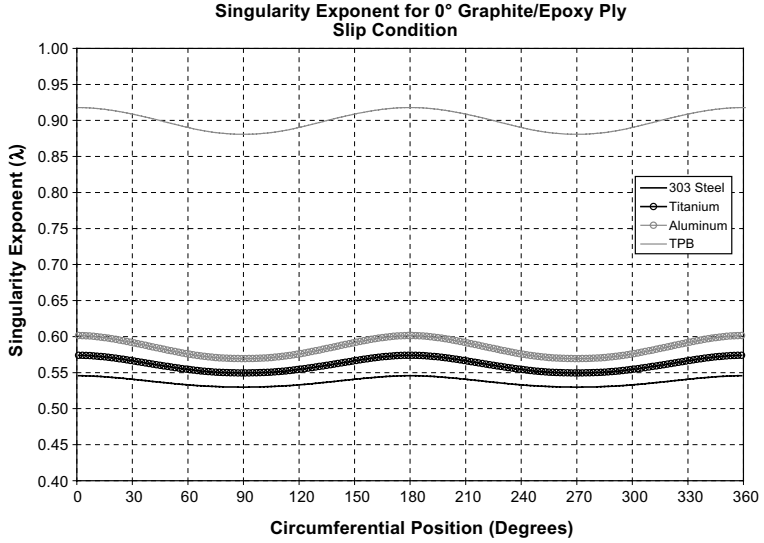

Fig. 6. Variation of singularity exponent.

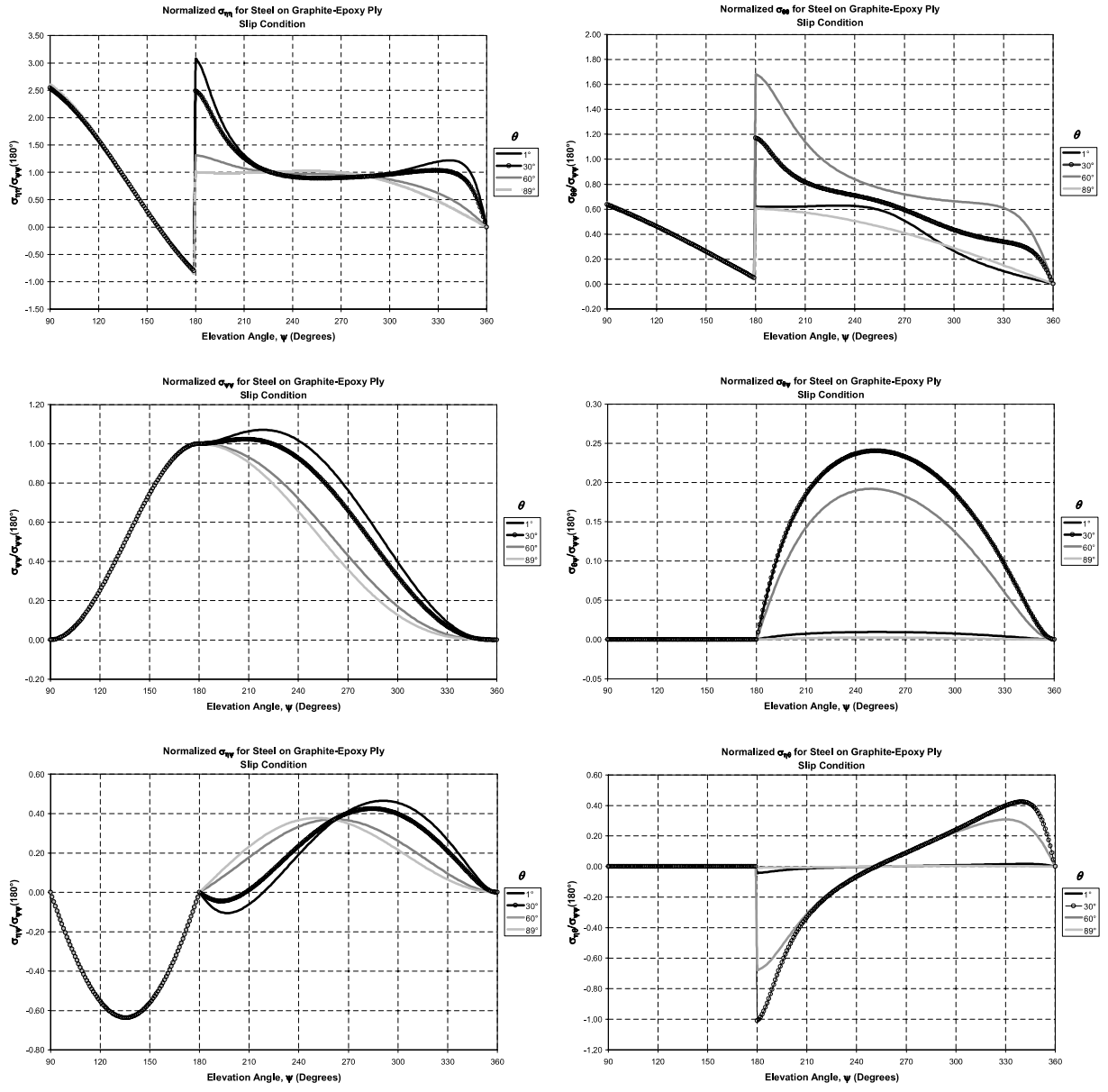

Fig. 7. Stress amplitudes for steel on 0° ply, slip condition, $\theta = 150°$.

the $\psi = 180°$ interface and zero at the free boundaries $\psi = 90°$, 360°; the transverse shear stress $\bar{\sigma}^{(1)}_{\psi\eta}(\lambda_1, \psi, \theta)$ is zero at all three surfaces $\psi = 90°$, 180° and 360°. A common feature evident all the stress components is that their amplitude inside the isotropic bolt-head is practically independent of the circumferential position, whereas inside the orthotropic plate it exhibits strong dependency upon θ. At the same time the shear stress components $\bar{\sigma}^{(1)}_{\psi\theta}(\lambda_1, \psi, \theta)$ and $\bar{\sigma}^{(1)}_{\eta\theta}(\lambda_1, \psi, \theta)$ are also very small inside the bolt-head.

Table 2
Geometric parameter values for full-field analysis cases

Symbol	Description	Value (mm)
d	Bolt head diameter	9.525
D_{bolt}	Bolt shank diameter	6.35
D_{hole}	Hole diameter	6.35
t_{bh}	Bolt Head thickness	6.35
δ_y	Bolt shank displacement (clamp-up)	8.333×10^{-4}
H	Plate thickness	12.70
X_{L}	Plate length	152.4
Y_{L}	Plate width	76.20
x_{c}	Hole-center x-position	76.20
y_{c}	Hole-center y-position	38.10

3.2. Numerical analysis and calculation of multiplicative coefficient $S_1(\theta)$

The multiplicative coefficient $S_1(\theta)$ at specific circumferential positions (θ-locations) was calculated by comparing the far-field solution to the asymptotic solution at a given radial distance from the singular point. A double-lap (symmetric against $z = 0$) plane bearing loading problem under boundary conditions (1) is considered. The bolt head and plate dimensions are given in Table 2. The applied displacement was $u_0 = 0.1524$ (1000 με). Circumferential location $\theta = 150°$ and steel bolt-head material will be chosen for detailed stress comparison. Two dimensionless (normalized by hole radius) radial distances from the singular contour were examined, $\eta = 0.00167$ and 0.00333. The asymptotic and numerical solutions at the described locations are compared in Fig. 8. Excellent agreement between the two solutions for all stress components was achieved by setting $S_1(150°) = -11.18$. It is worth mentioning that due to the strong character of the singularity the influence of the non-singular terms in the series (17) is quite small compared to the case with weak singularities (Iarve, 1997). This property manifests itself in the fact that, with exception of $\sigma_{\theta\theta}$ (constant additive term = 10), no constant additive terms were added to the one-term asymptotic expansion to obtain good agreement with the full-field numerical solution.

Fig. 9 displays $S_1(\theta)$ as a function of circumferential coordinate in the bearing–loading problem under consideration. Based on the comparisons presented above, one stress component ($\sigma_{\psi\eta}$) was used at $\eta = 0.00167$ to determine the multiplicative factor of the singular term. The curve is symmetric due to the large preload applied to the fastener relative to the bearing load. If the preload was smaller, non-uniform distribution of clamping stress would result in an unsymmetric appearance in Fig. 9. It is hoped that the quantity $S_1(\theta)$ can be used to predict failure initiation at the bolt-head edge under general loading conditions.

4. Conclusions and recommendations

Singular stresses arising in the neighborhood of frictionless contact surfaces introduced in laminated orthotropic plates by mechanical joining with clamp-up were investigated by using local asymptotic solutions and full-field numerical analysis. Three-dimensional B-spline approximation of displacements and a penalty function-based contact solution was used for numerical analysis. Clamping loads are included in the analysis.

The present study has examined specific combinations of bolt-head and composite plate materials that represent a range of materials and relative stiffnesses encountered in practical applications. It was found that the characteristics of the stress singularity for such practically important combinations as titanium bolt-head/carbon fiber composite plate are similar to that of a crack in terms of the power of singularity and uniqueness of the singular term.

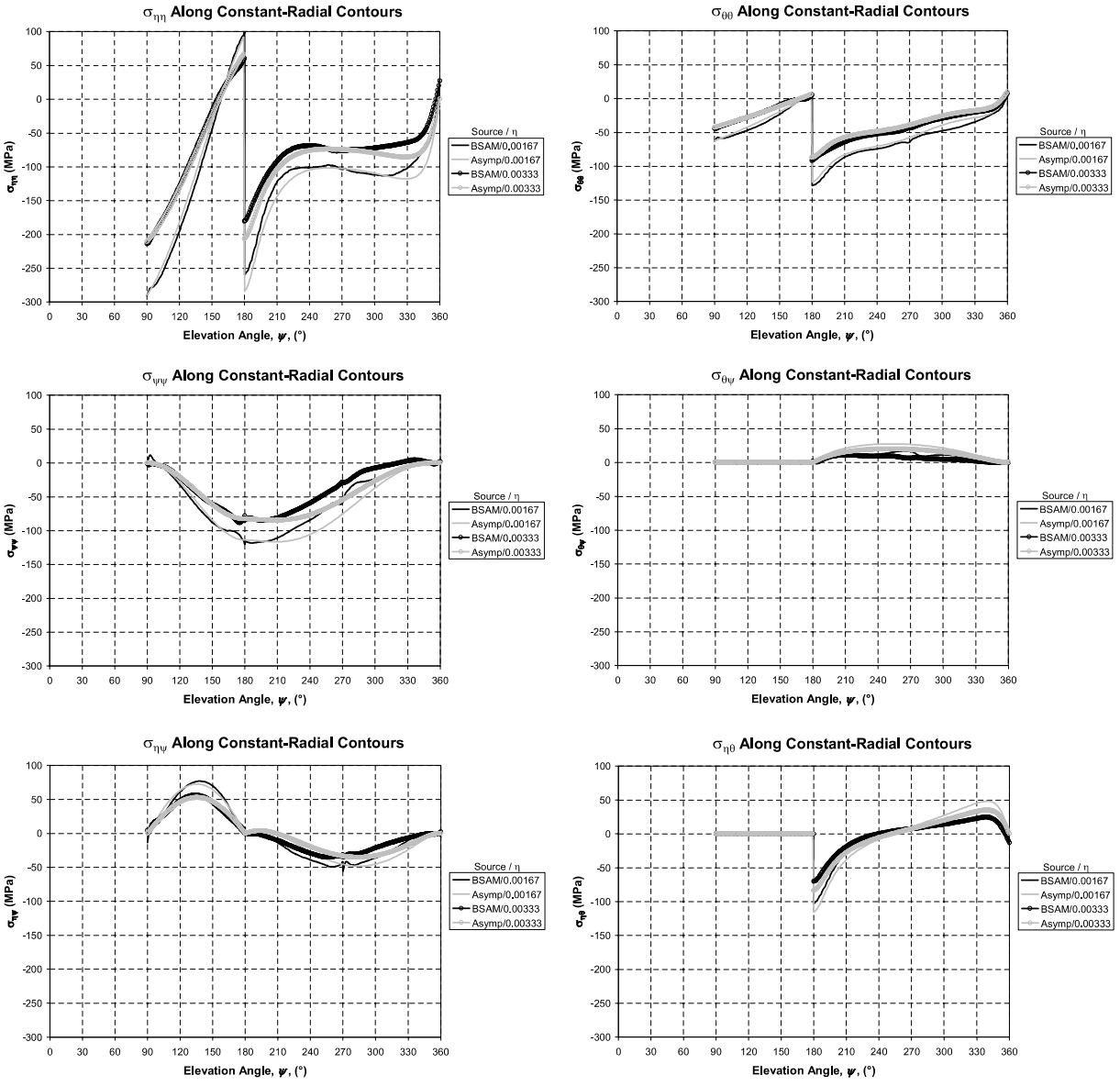

Fig. 8. Comparison of numerical and asymptotic solutions at $\theta = 150°$.

Comparison of all stress components in the vicinity of the singular contour was performed between the full-field numerical solution and the singular asymptotic solution. Excellent agreement was observed allowing for reliable determination of the unknown multiplicative factor. The distribution of the multiplicative factor of the singular stress amplitude as a function of circumferential coordinate in the double-lap bearing problem with clamp-up was obtained.

In view of the similarities in character of the singular stress behavior at the bolt-head edge to that of a crack in linear-elastic fracture mechanics, experimental work to further investigate whether a single parameter $S_1(\theta)$ can be validated to control the bolt-head edge shear-in failure is recommended.

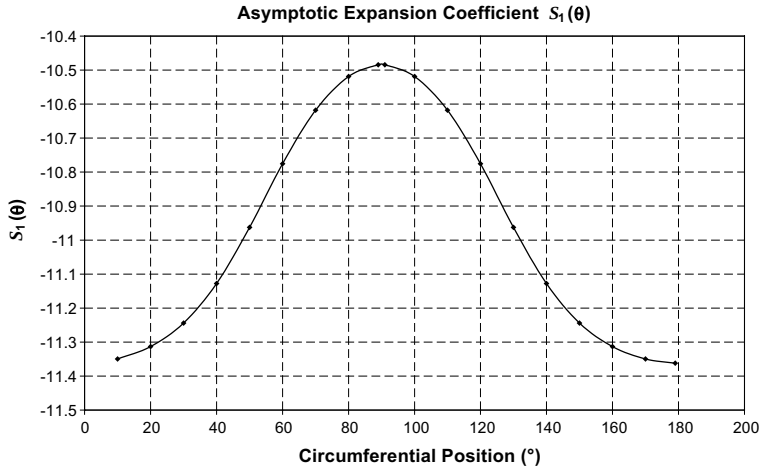

Fig. 9. Variation in asymptotic expansion coefficient.

Acknowledgements

The work was sponsored by the Air Force Research Laboratory, under contract number F33615-00-D-5006. Support of the first author from the Dayton Area Graduate Studies Institute also is gratefully acknowledged.

Appendix A

$$\mathbf{F}=\left[\begin{array}{c|c|c} C_{11}\cos^2\theta+ 2C_{16}\sin\theta\cos\theta+ C_{26}\sin^2\theta & C_{12}\cos\theta\sin\theta+ C_{62}\sin^2\theta+ C_{16}\cos^2\theta+ C_{66}\cos\theta\sin\theta & C_{14}\cos\theta\sin\theta+ C_{64}\sin^2\theta+ C_{15}\cos^2\theta+ C_{65}\cos\theta\sin\theta \\ \hline C_{12}\cos\theta\sin\theta+ C_{62}\sin^2\theta+ C_{16}\cos^2\theta+ C_{66}\cos\theta\sin\theta & C_{22}\sin^2\theta+ 2C_{26}\sin\theta\cos\theta+ C_{66}\cos^2\theta & C_{64}\cos\theta\sin\theta+ C_{24}\sin^2\theta+ C_{65}\cos^2\theta+ C_{25}\cos\theta\sin\theta \\ \hline C_{14}\cos\theta\sin\theta+ C_{64}\sin^2\theta+ C_{15}\cos^2\theta+ C_{65}\cos\theta\sin\theta & C_{64}\cos\theta\sin\theta+ C_{24}\sin^2\theta+ C_{65}\cos^2\theta+ C_{25}\cos\theta\sin\theta & C_{44}\sin^2\theta+ 2C_{45}\sin\theta\cos\theta+ C_{55}\cos^2\theta \end{array}\right]$$

$$\mathbf{G}=\begin{bmatrix} 2\begin{pmatrix} C_{15}\cos\theta+ \\ C_{56}\sin\theta \end{pmatrix} & \begin{matrix}(C_{25}+C_{46})\sin\theta+ \\ (C_{14}+C_{56})\cos\theta\end{matrix} & \begin{matrix}(C_{36}+C_{45})\sin\theta+ \\ (C_{13}+C_{55})\cos\theta\end{matrix} \\ \begin{matrix}(C_{25}+C_{46})\sin\theta+ \\ (C_{14}+C_{56})\cos\theta\end{matrix} & 2\begin{pmatrix} C_{46}\cos\theta+ \\ C_{24}\sin\theta \end{pmatrix} & \begin{matrix}(C_{23}+C_{44})\sin\theta+ \\ (C_{36}+C_{45})\cos\theta\end{matrix} \\ \begin{matrix}(C_{36}+C_{45})\sin\theta+ \\ (C_{13}+C_{55})\cos\theta\end{matrix} & \begin{matrix}(C_{23}+C_{44})\sin\theta+ \\ (C_{45}+C_{36})\cos\theta\end{matrix} & 2\begin{pmatrix} C_{35}\cos\theta+ \\ C_{34}\sin\theta \end{pmatrix} \end{bmatrix}$$

$$\mathbf{H}=\begin{bmatrix} C_{55} & C_{45} & C_{35} \\ C_{45} & C_{44} & C_{34} \\ C_{35} & C_{34} & C_{33} \end{bmatrix}$$

References

Bar-Yoseph, P., Avrashi, J., 1988. On the nature of the free edge stress singularity in composite laminated plates. International Journal for Numerical Methods in Engineering 26 (7), 1507–1523.

Ericson, K., Persson, M., Carlsson, L., Gustavsson, A., 1984. On the prediction of the initiation of delamination in a [0/90]s laminate with a circular hole. Journal of Composite Materials 18, 495–506.

Eriksson, I., 1990. On the bearing strength of bolted graphite/epoxy laminates. Journal of Composite Materials 24, 1246–1269.

Folias, E.S., 1989. On the interlaminar stresses of a composite plate around the neighborhood of a hole. International Journal of Solids and Structures 25 (10), 1193–1200.

Folias, E.S., 1992. Boundary layer effects of interlaminar stresses adjacent to a hole in a laminated composite plate. International Journal of Solids and Structures 29 (2), 171–186.

Gerald, C.F., Wheatley, P.O., 1994. Applied Numerical Analysis. Addison-Wesley Publishing Co, Reading, MA.

Iarve, E.V., 1996. Spline variational three-dimensional stress analysis of laminated plates with open holes. International Journal of Solids and Structures 33 (14), 2095–2118.

Iarve, E.V., 1997. Three-dimensional stress analysis in laminated composites with fasteners based on the B-spline approximation. Composites—Part A: Applied Science and Manufacturing 28 (6), 559–571.

Iarve, E.V., 2000. Asymptotically exact stresses in laminates with a rigid fastener. Composite Science and Technology 60, 2365–2374.

Iarve, E.V., Mollenhauer, D.H., 2002. Full-field singular stresses in a composite laminate weakened by a cylindrical cavity: theory and experiment. Advanced Composite Materials 11, 21–29.

Iarve, E.V., Pagano, N.J., 2001. Singular full-field stresses in composite laminates with open holes. International Journal of Solids and Structures 38 (1), 1–28.

Mikhailov, S.E., 1978. A plane problem for two bonded anisotropic wedges. Izvestiya Akademii Nauk SSSR, Mekhanika Tverdogo Tela (4), 155–160.

Mikhailov, S.E., 1979a. A stress singularity in the region of a rib in a composite inhomogeneous anisotropic body and some applications to composites. Izvestiya Akademii Nauk SSSR, Mekhanika Tverdogo Tela (5), 103–110.

Mikhailov, S.E., 1979b. A stress singularity in a compound arbitrarily anisotropic body, and application to composites. Izvestiya Akademii Nauk SSSR, Mekhanika Tverdogo Tela (6), 33–42.

Oplinger, D.W., 1996. Bolted joints in composite structures—an overview. In: 83rd Meeting of the AGARD Structures and Materials Panel, Florence, Italy.

Press, W.H., Flannery, B.P., Teukolsky, S.A., Vetterling, W.T., 1989. Numerical Recipes: The Art of Scientific Computing. Cambridge University Press, Cambridge, UK.

Reedy Jr., E.D., 1989. On free-edge interlaminar stress distributions. Composites Science and Technology 34 (3), 259–266.

Smith, P.A., Pascoe, K.J., Polak, C., Stroud, D.O., 1986. Behaviour of single-lap bolted joints in CFRP laminates. Composite Structures 6, 41–55.

Stolarski, H.K., Chiang, M.Y.M., 1989. On the significance of the logarithmic term in the free edge stress singularity of composite laminates. International Journal of Solids and Structures 25 (1), 75–93.

Wang, S.S., Choi, I., 1982. Boundary-layer effects in composite laminates: Part 1—free-edge stress singularities. Journal of Applied Mechanics 49, 541–559.

Wang, S.S., Lu, X., 1993. Three-dimensional asymptotic solutions for interlaminar stresses around cutouts in fiber composite laminates. In: Mechanics of Thick Composites. Applied Mechanics Division of ASME, New York.

Wang, S.S., Yuan, F.G., 1983. A hybrid finite element approach to composite laminate elasticity problems with singularities. Journal of Applied Mechanics 50 (4A), 835–844.

Whitney, T.J., Iarve E.V., 2002. Three-dimensional spline-based stress analysis of bolted composite joints with clamping. In: Proceedings of the American Society for Composites 17th Technical Conference, West Lafayette, IN.

Yang, B., Pan, E., Yuan, F.G., 2003. Three-dimensional stress analyses in composite laminates with an elastically pinned hole. International Journal of Solids and Structures 40 (8), 2017–2035.

Zwiers, R.I., Ting, T.C.T., Spilker, R.L., 1982. On the logarithmic singularity of free-edge stress in laminated composites under uniform extension. Journal of Applied Mechanics 49, 561–569.